Master’s thesis 2016

Study of the interaction between HSV-1 and a native-like supported lipid bilayer with total internal reflection fluorescence microscopy

ENEAS SCHMIDT

CHALMERS

Department of Physics

CHALMERS UNIVERSITY OF TECHNOLOGY

Gothenburg, Sweden 2016

Abstract

Viruses pose a great threat to human health because many viral diseases have no cure to this day and new viruses are likely to emerge in the future. There is therefore a continuous need for the development of vaccines and anti-viral pharmaceuticals. Moreover, platforms making it possible to measure the effectiveness of potential antiviral drugs are urgently needed to accelerate the development progress of antiviral drugs. The available screening systems today are often either cell-based systems or basic interaction platforms. Accordingly they are either expensive or very simplified. A new approach to antiviral drug screening, in particular in the context of virus binding inhibitors, that is cheaper and easier to maintain compared to cell-based systems but still preserves some of the complexity of a native system, is an *in vitro* platform based on native-like supported lipid bilayers (SLBs). Such a system focuses on the interaction of the virus with the cell membrane, and the inhibition of this interaction to prevent infection.

In this project, an *in vitro* screening platform for use with the herpes simplex virus (HSV) was developed, based on the extraction of native membrane material from green monkey kidney (GMK) cells. Association and dissociation events between fluorescently labeled herpes simplex virus type 1 (HSV-1) and native membrane SLBs were examined with total internal fluorescence (TIRF) microscopy. The binding kinetics could be extracted with equilibrium fluctuation analysis, a method based on the observation of the binding and release process of individual virus particles. As a first application of this platform, a mutant strain of HSV-1 lacking the membrane bound glycoprotein C (gC), a ligand that facilitates the attachment to native membranes was compared to the wildtype HSV-1 KOS strain. As expected, the results showed that that the gC deficient strain had significantly less binding compared to the wildtype. Additionally an inhibition study was performed with the glycosaminoglycan (GAG) heparin to determine its effect on binding. The heparin inhibition study revealed a dose dependent inhibitory response. The results demonstrate the functionality of the platform and its ability to measure specific binding interactions. This shows the potential of the sensor platform to be used as a bioanalytical screening tool for antiviral drug testing.

Table of Contents

1

Introduction

Viruses are small parasite particles that can infect all living organisms, causing in many cases diseases. They are not capable of replicating on their own; instead they rely on the cell machinery of their targets. Viruses contain genetic material, either RNA or DNA, which can be single or double stranded. Once infected, the target cells produce proteins and replicate the genetic material leading to the formation of new viral copies which exit the cell to continue their life cycle (Lodish and Darnell, 2000). There is currently no cure for many viral diseases. Therefore, the development of new drugs and vaccines widely relies both on understanding the entire mechanism of cell infection and on the development of methods for an efficient screening of antiviral drugs. In this context, the cell membrane separating the interior of the cell from the extracellular environment plays a key role because viral attachment and entry is the first crucial step towards infection. The importance of understanding the cell membrane is further reflected by the fact that the majority of pharmaceuticals today are targeted against membrane proteins (Josic and Clifton, 2007). The development of a native-like model system for evaluation of candidate drugs would greatly contribute to progress in pharmaceutical research.

Supported Lipid bilayers (SLBs) are membranes produced artificially by self-assembly of lipids and deposited onto a solid support. Their composition is close to that of living cells but they have the advantage of being a simpler system that can be studied with surface sensitive techniques (Moller and Seeger, 2015). Naturally, SLBs can be used to study the structure and functionalities of the membrane (Gozen and Jesorka, 2012) but they may also be used in biochips to preserve the structure and functionality of membrane proteins as a biosensing platform in drug development (Bally et al., 2010). Binding studies carried out exclusively with individual receptor ligand pairs are the simplest system to investigate biomolecular interactions. However in such a simplified system, the complexity that contributes to the native behavior of the membrane components is not taken into account, calling for the development of assays taking advantage of a more native-like membrane composition (Koshy and Ziegler, 2015). Previous iterations of SLBs with functional and mobile membrane proteins have used simplified compositions, including only one or a few components. However, in 2015 Pace *et al.* (Pace H. et al) proposed an alternative construction of native-like SLBs assembled from native membranes and synthetic vesicles. The synthetic vesicles modified with a polymer keep the membrane proteins from laying directly onto the glass substrate because of a PEG-related cushioning effect (Pace et al., 2015). The construction of these hybrid SLBs allow for the development of a new type of platform for antiviral screening.

1.1 Aim

The goal of this project was to build and characterize native-like SLBs produced by vesicle fusion and then probe the interaction between the SLBs and herpes simplex virus type 1 (HSV-1). The SLBs were constructed of native membranes from a cell line relevant to HSV-1 infection called green monkey kidney (GMK) and synthetic PEG-POPC vesicles. To gain insights into the contribution of different biomolecules to the interaction kinetics and to test the functionality of the platform, the binding behavior of a mutant HSV-1 strain lacking the main attachment glycoprotein (gC) will be compared to the wildtype strain. Additionally, the inhibitory effect of the glycosaminoglycan (GAG) heparin will be evaluated. The binding kinetics will be assessed using equilibrium-fluctuation analysis and the imaging will be performed with time-dependent total internal reflection fluorescence (TIRF) microscopy.

2

Background & Theory

In this chapter, the reader is familiarized with the basic components of the platform and the theory behind the techniques used in the study. First, an introduction is given to the biology of the cell plasma membrane and the structure of HSV. Following is a description of the kinetical models utilized. In the second part the theory of the methods used in the experimental study are described in detail.

2.1 Background to biology

To understand how the different components of the platform interact with each other, it is important to have both some basic insights. The structure and functions of the biomolecules found in the membrane but also on the kinetic models describing the association and dissociation interactions between ligand and receptor are provided in this chapter.

2.1.1 The cell membrane and its components

The plasma membrane's primary function is to separate the inside of the cell from the external environment. Beyond protecting the cell, the membrane is also involved in a number of essential functions, in particular in the context of mediating communication with the cell's surroundings. The basic structure of the plasma membrane is a lipid bilayer carrying a multitude of membrane proteins and sugars. The bilayer consists of different amphiphilic lipids that have a hydrophilic head and a lipophilic tail. They can spontaneously form a bilayer by positioning themselves in an ordered manner effectively separating the outside from the inside of the cell, see Figure 1.

There are several thousands of different lipids in the eukaryotic cell determining membrane function and structure. They can be categorized in three main groups: phospholipids, cholesterol and glycolipids (van Meer et al., 2008). Phospholipids are perhaps the most fundamental component of the plasma membrane, as it defines the basic architecture of the

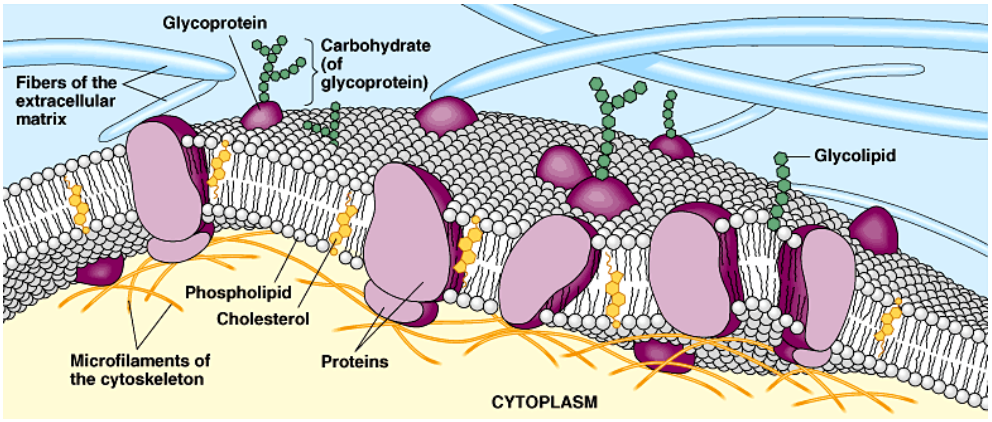

***Figure 1**: The simplified structure of the plasma membrane. The phospholipid bilayer separates the cell cytoplasm from the outside environment. The three main components of the membrane are lipids, proteins and carbohydrates. http://cmapspublic3.ihmc.us.*

membrane. Cholesterol provides rigidity to the structure and glycolipids are lipids with an attached carbohydrate that appears on the exterior surface of the membrane that for example helps with cellular recognition.

Membrane proteins are enormously diverse and have an even wider range of functions. There are peripheral membrane proteins, which are bound to the membrane but are completely water soluble; there are also integral membrane proteins which span across the hydrophobic core of the membrane. Membrane proteins are important for cell signaling and attachment, transport of molecules through membranes or intracellular cytoskeletal connections, among other things.

In addition to protein and lipids, carbohydrates are responsible for several important functions in the plasma membrane; glycolipids are lipids that have one or several monosaccharides attached to it, proteoglycans are proteins with carbohydrates attached and finally there are proteoglycans, large molecules consisting of a core protein decorated with GAGs which is the most notable carbohydrate in this project. GAGs are present in all mammalian cells; they are large linear polysaccharides that structurally consist of repeating disaccharide units. GAGs are highly sulfated making them very negatively charged. The only exception to this is hyaluronic acid. They are attached to the outer cell membrane, able to bind large amounts of water forming a gel structure that is protective but also assists in cell adhesion and binds and regulates a large number of proteins, one being adhesion molecules (Gandhi and Mancera, 2008). Of direct relevance to this project, GAGs work as attachment factors for the viral glycoproteins of HSV responsible for the initial attachment to the cell surface.

2.1.2 Herpes Virus Type 1

Herpes simplex type I (HSV-1) is a very widespread human virus around the world; a global study estimated that 67% of all people under the age of 50 were infected in 2012 (Looker et al., 2015). The HSV-1 is a virus that most commonly causes oral infections known as cold sores in and around the mouth. The infection can, in rare cases, cause acute brain inflammation and corneal infection, more frequently occurring among infants. The infection is chronic meaning that it cannot be cured. Rather, the virus remains latent in the sensory ganglia until the symptoms return (Krug et al., 2004).

Herpes simplex type 1 (HSV-1) is an enveloped DNA virus with a structure described in Figure 2. The double stranded DNA is located in the center of the virus and is surrounded by a capsid made of protective proteins called capsomeres. Outside of the capsid is yet another layer of protective proteins that is present in all herpes viruses and that is known as tegument or viral matrix (Yu et al., 2011). Finally, HSV-1 has a lipid envelope surrounding the capsid. This membrane originates from the host cell and contains mainly viral glycoproteins and envelope proteins that are important for cell attachment and entry (Spear, 2004).

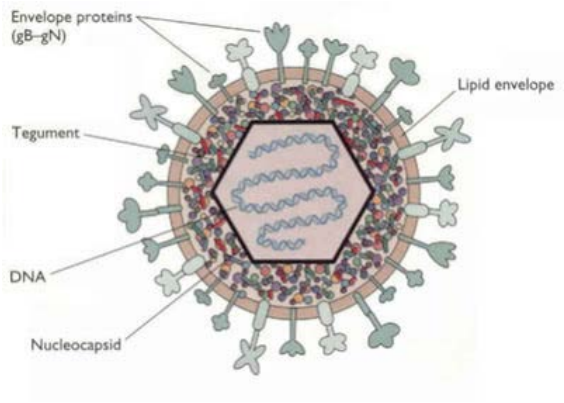

***Figure 2**: The basic composition of HSV-1. The dsDNA is encapsulated by a protein capsid (called nucleocapsid in this illustration). The capsid is further coated with a layer of protective proteins called tegument. Finally a lipid envelope containing a number of glycoproteins surrounds the tegument. HSV-1 is designed to attach and fuse to the lipid membrane and release its DNA into the target cell. viralinfections.info*

HSV-1 enters the cell by recognizing receptors on the cell surface followed by fusion with the host cell membrane. There are several glycoproteins on the viral surface and receptors in the target cell membrane that are involved in the mechanism of attachment and entry. The glycoproteins gC and gB are believed to bind to the sulfated GAGs on proteoglycans, especially heparan sulfate and chondroitin sulfate which act as attachment receptors for the viral glycoproteins on the membrane (Spear, 2004). The initial attachment facilitates the cell entry by confining other glycoproteins responsible for membrane fusion to the surface. It is understood that at least three glycoproteins are responsible for viral entry: gD and gH-gL. The initial binding of gC and gB to heparan sulfate (HS) is important for the following cell entry but not essential. It has been shown that a HSV-1 strain lacking the glycoprotein gC exhibit a reduced the infectivity by a factor of ten (Herold et al., 1991).

2.2 Kinetics of ligand-receptor interactions

To understand the data acquired in this thesis, we consider the case of a ligand in solution binding to a receptor immobilized on a surface. In this case, the reaction rate is either limited by the diffusion of the ligands to the receptor, in a case called diffusion limited reaction, or, by the reaction itself which depends on the rate of reaction between the ligand and receptor (reaction limited regime). A simple model is usually good enough to provide a general view of the system under investigation (Dahlin, 2012).

The change in surface coverage in a system with reversible binding and reaction-limited kinetics at a surface can be described by the differential equation below based on the Langmuir model:

$$\frac{\partial \Gamma(t)}{\partial t} = K_{on} \times C\left(\Gamma_{max} - \Gamma(t)\right) - k_{off} \times \Gamma(t) \qquad [2.1]$$

Where $\Gamma(t)$ is the surface concentration of the ligand-receptor complex and Γ_{max} is the maximum coverage of receptor, bound or not bound to a ligand. The two reaction-coefficients k_{on} and k_{off} are constants that describe the rate of binding and release. They have different units depending on the system. It is assumed that the supply of ligands that bind to the receptors is constant at the surface; by doing this, the concentration of ligands in bulk can be described by a constant C. If the system is allowed to reach a steady-state, meaning $t \rightarrow \infty$ and

the association boundary condition $\Gamma(0) = 0$ is met, the Langmuir isotherm equation can be described as:

$$\frac{\Gamma_{eq}}{\Gamma_{max}} = \frac{C}{C+\frac{k_{off}}{k_{on}}} = \frac{C}{C+K_D} \quad [2.2]$$

Where $\Gamma_{\text{equilibrium}} / \Gamma_{max}$ is the fractional coverage which can be described by C and the dissociation constant K_D, the latter is defined as k_{off}/k_{on} or as C_AC_B/C_{AB} for the general reaction $C_A+C_B \rightarrow C_{AB}$. Because of this relation, plotting the fractional coverage against the concentration C gives the equilibrium dissociation constant at 50% coverage.

If we instead look at the dissociation boundary condition where the concentration of ligand is depleted and the surface coverage is equilibrated, $\Gamma(0) = \Gamma_{eq}$ and $C = 0$, equation [2.3] describes the exponential decay of bound ligands the following way:

$$\Gamma(t) = \Gamma_{eq} e^{-k_{off}t} \quad [2.3]$$

If the ligands diffuse slowly they will start to deplete close to the surface in which case the system becomes diffusion limited. In this situation the kinetics cannot be described by the Langmuir model any longer, instead the Ilkovic equation define the system:

$$\Gamma(t) = 2C_0\sqrt{\frac{Dt}{\pi}} \quad [2.4]$$

Where D is the diffusion coefficient of the ligand and C_0 is the bulk concentration of the ligand. In this model the reaction is irreversible. The Ilkovic model is a good model to describe the ligand binding behavior in a diffusion-limited reaction but only before equilibrium conditions because the $\Gamma(t)$ term never converges. The Ilkovic model should simply not be used after equilibrium conditions are met, but should instead be described by Langmuir at this point.

It should be noted that binding reactions are often complex and that a kinetic model that is completely reaction or diffusion limited cannot necessarily describe kinetics entirely accurately because in reality reactions depend on both mass transfer and reaction rate.

2.3 Theoretical Background on the Experimental Techniques

In this section, the techniques used to study lipid mixing and ligand-receptor interactions are described.

2.3.1 Supported lipid bilayer formation and vesicle fusion

In an attempt to create a simplified model of the cell membrane and to study membranes closely, so-called supported lipid bilayers (SLBs) have been widely used. An SLB is a lipid bilayer that rests on a solid support, which is typically silica, mica or glass depending on the technique used to study its function. SLBs have been used to analyze the membrane's complexity and mechanical properties with atomic force microscopy (AFM) or with surface sensitive techniques that take advantage of an evanescent field such as TIRFM and surface plasmon resonance (Lin et al., 2006). They have also been used to immobilize membrane proteins at sensing interfaces while preserving their functionality; membrane proteins need their native environment to preserve structure and function, making it difficult to study them otherwise. SLBs can be formed in many different ways, vesicle fusion being a commonly

used simple method. This method is based on the spontaneous rupturing of small vesicles, lipid bilayer spheres that enclose a liquid inside them, when in contact with a surface, see Figure 3

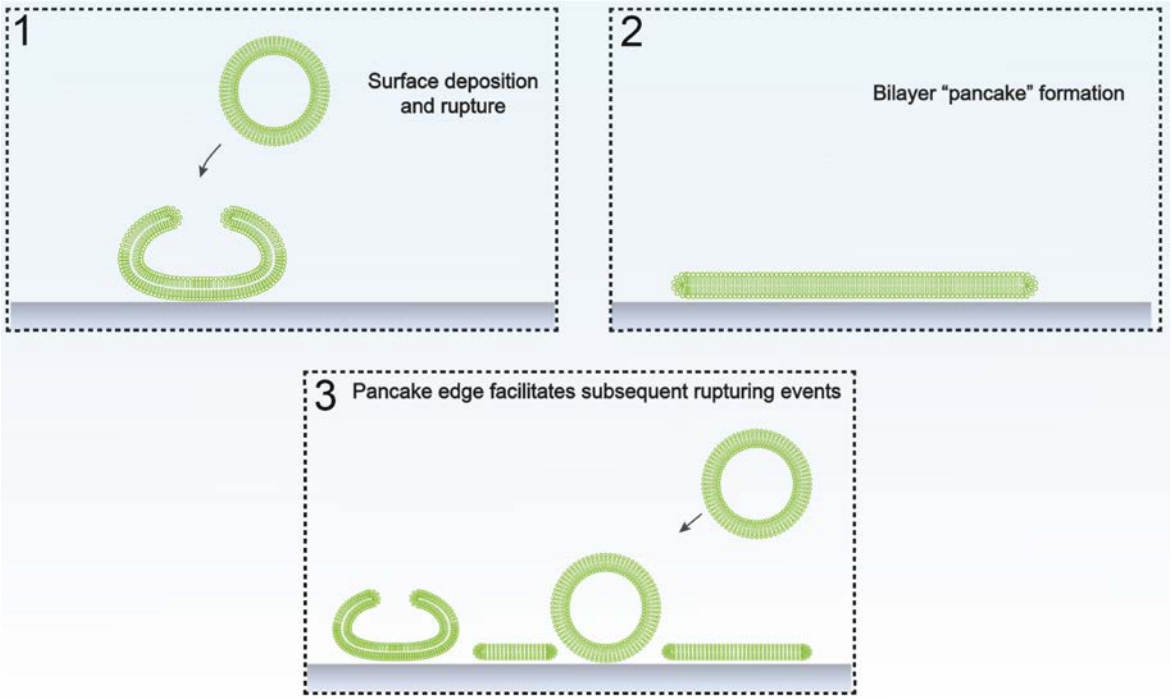

***Figure 3**: The process of vesicle fusion on a solid support. (1) Vesicles are attaching to the surface and ruptures. (Karre and Cooper) The membrane starts to spread on the surface forming a pancake structure. (3) High energy edges are fusing spontaneously eventually forming a continuous SLB. Figure credit goes to Silver Jõemetsa.*

In theory, surface-induced vesicle fusion is divided into two steps, the first being vesicle adhesion and crowding. During this step, the vesicles adsorb to the solid support but they are usually not rupturing on their own because of the rigidity of the membrane. As more vesicles attach to the surface more and more vesicles are interacting and a critical vesicle surface coverage is eventually reached leading to the initiation of vesicle fusion. The edges of the ruptured vesicles then spread on the surface eventually leading to a continuous bilayer. How well the vesicles rupture depends on several parameters such as pH and ionic strength, but also on the composition of the vesicles themselves. Generally, pH and ionic strength can be tuned in order to reduce electrostatic repulsion or increased attraction between the surface and the vesicle to facilitate vesicle rupture.

SLBs used in biophysical studies can vary a lot in complexity. The early studies on SLBs mimicked the simplest structure of a plasma membrane using only a few types of lipids. However for more complex studies of biological function more native components, including membrane proteins need to be incorporated. At the end of the complexity scale, recent publications show that a whole native membrane, including proteins and carbohydrates can be incorporated into SLBs (Pace et al., 2015, Richards et al., 2016). The latter has been proven widely challenging. Indeed while some of the most common lipids in the plasma membrane and in particular phosphocholine lipids (for example POPC) are known to form SLBs very easily, it is not energetically favorable for all membranes to form SLBs. Protein density and lipid composition are factors that directly influence the formation of SLBs on a substrate. In particular, native membranes have a complex composition and include molecules such as

cholesterol, which makes the membranes more rigid and less likely to rupture on a solid support. The membranes also contain a variety of proteins that do not facilitate SLB formation. In short, an increased complexity of the membrane complicates the vesicle rupture and the subsequent SLB formation (Simonsson et al., 2011). Thus, the challenge becomes to incorporate as much native material as possible so that a satisfactory SLB may still be formed. It can be advantageous to make hybrid vesicles of native and synthetic vesicles to facilitate the SLB formation and this method has been shown to be successful. Pace H. et al, 2015 described a technique also used in this work to form native membrane SLBs by first creating hybrid vesicles of native membrane vesicles (NMVs) extracted from cells and synthetic PEGylated POPC vesicles by ultra-sonication. The hybrid vesicles were able to form SLBs spontaneously on a glass substrate while simultaneously keeping the proteins mobile inside the bilayer (Pace et al., 2015). Using a different approach Richards M. et al made native membrane SLBs by simultaneously adsorbing PEGylated POPC vesicles and native membrane cell blebs onto a glass substrate without the requirement of formation of hybrid vesicles in advance. This method has the advantage of preserving the orientation of the membrane proteins (Richards et al., 2016).

There are a handful of techniques that are generally used to study the formation, structure and function of SLBs. The most commonly used method to study SLB formation is quartz crystal microbalance with dissipation monitoring (QCM-D). This method makes it possible to measure the sample average mass change and changes in viscoelastic properties during SLB formation. Monitoring the latter can help elucidate if SLBs are formed or not. This is because vesicles are elastic while bilayers are rigid making them easy to discriminate (Richter and Brisson, 2005). QCM-D does however not provide imaging. Atomic force microscopy (AFM) is a scanning probe microscope that uses a vibrating cantilever to measure the topography of a surface, which can yield valuable information on the morphology of the bilayer (Richter et al., 2003). Fluorescence microscopy is another imaging method that has the advantage of being able to image single molecules. This technique can image the formation of SLBs by probing the vesicle fusion of single fluorescent vesicles. With TIRF microscopy it is also possible to examine the association and dissociation behavior of single molecules to the SLBs that is essential for an investigation of binding kinetics.

2.3.2 Fluorescence microscopy

Fluorescence microscopy is a microscopy technique that has attracted considerable interest in the context of biology and in life sciences. It is widely used to study biological samples because of its increased contrast capabilities compared to traditional brightfield microscopy. This technique is based on labeling specific molecules with fluorescent markers, called fluorophores, so that they can be distinguished from other components. Furthermore, objects smaller than the diffraction limit can be localized which is of great interest in biomedical sciences and biology. Fluorescence microscopy takes advantage of a phenomenon called fluorescence.

Fluorescence is a physical phenomenon where a molecule or atom is excited from the ground state into a non-stable excited state; when it returns to its ground state the excess energy is then released as light.

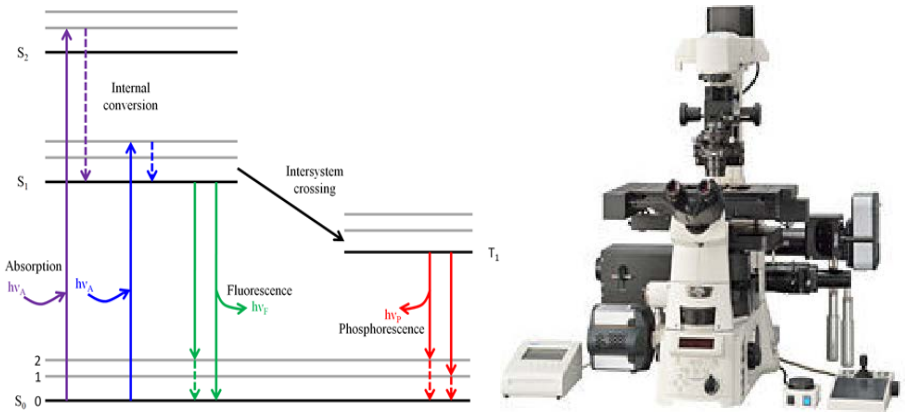

(A) (B)

***Figure 4**: (A) In a Jabłoński diagram the energy levels are described as ground state (S0) and excited states (Sn). Energy can be released as fluorescence or via intersystem crossing and phosphorescence depending on the fluorescent molecule. nptel.ac.in/courses/102103044/6 (B) A fluorescent microscopy capable of using TIRF.*

The action of fluorescence begins with the excitation of an electron into one of the singlet excited states (S_n) depending on the energy absorbed. If the energy is higher than the lowest singlet state (S_1) an internal conversion releases the energy difference between the two levels. The energy levels of the electrons in the excited state quickly lose excess energy by non-radiative transition, which includes vibrational relaxation, rotation and heat generation. Once the energy of the electron is at the lowest possible sublevel in the S_1 state the excess energy will be emitted by light. The energy of the emitted light is expectedly at a lower energy than the initial excitation, this energy reduction is called the “stokes shift” and it is different for every fluorophore. The whole process is illustrated in the Jabłoński diagram, see Figure 4A.

A fluorophore is a molecule that has an energy difference between its ground state and the first excited state that corresponds to the photon energy of visible light. In fluorescence microscopy, a fluorophore may be attached to a molecule, which greatly increases its visibility, making it possible to discriminate different molecules from each other and this has been proven to be extremely valuable in biological science. The energy difference between the excitation and emission light is very suitable for the purpose of microscopy since the excitation and emission can be discriminated inside the microscope by an emission filter. The microscope can pick up the emitted light at the right wavelength and avoid any interference with the incident light (Ishikawa-Ankerhold et al., 2012). Figure 4B is the inverted fluorescence microscope used in this project.

2.3.3 Total Internal Fluorescence Microscopy

In this project, we take advantage of a special type of fluorescence microscopy called total internal reflection fluorescence microscopy (TIRF). TIRF is a microscopy technique that allows for greater contrast by increasing the signal to noise ratio compared to widefield fluorescence microscopy. This is achieved by only exciting fluorophores in close vicinity to the interface and hence effectively removing noise from out of focus fluorophores (Yamamura et al., 2015).

The working principle of TIRF is based on total internal reflection. Total reflection requires the propagating light to encounter a medium of lower refractive index than the other medium, for example light propagating through glass to water. In addition, the angle of the incident

light has to be above a so-called critical angle, for which all light is completely reflected. Total internal reflection on the interface leads to a generation of an evanescent field that has the same frequency as the incident light but that decays exponentially in the medium of lower refractive index. This evanescent field is used to illuminate the fluorophores in vicinity of the interface. The depth (d) of the evanescent field depends on the refractive indices (n) of the sample and microscope slide, the angle (θ) of the incident light and its wavelength (λ) (Ross et al., 2015).

$$d = \frac{\lambda}{4\pi} \times \left({n_{glass}}^2 \sin(\theta)^2 - {n_{sample}}^2 \right)^{-1/2} \quad [2.5]$$

Once the depth the evanescent wave is known, the energy (E) can be calculated for a certain distance from the interface, which has an exponential decay in the z-direction.

$$E(z) = E(0)e^{-\frac{z}{d}} \quad [2.6]$$

The range of fluorescence excitation is typically less than 100-200 nm thick in the z-direction, consequently illuminating only the fluorophores in that range. Due to the increased signal to noise ratio single particles or even single fluorophores can be studied at the interface.

Since the sample is required to have a lower refractive index than the glass, biological samples and hence also SLBs are perfectly suited for this technique because they mainly consists of water. TIRFM can also greatly enhance the quality of measurements on mobility of fluorescently labeled molecules because of the increased contrast at the interface.

In this project, TIRF microscopy is utilized to study the formation of supported lipid bilayers and also to visualize individual viruses as they bind to the hybrid SLBs. The kinetics of the system can be determined and compared for different conditions by observing the association and dissociation of particles.

2.3.4 Förster Resonance Energy Transfer

Förster (or Fluorescence) Resonance Energy Transfer (FRET) is a mechanism of energy transfer between two fluorophores, a donor and acceptor. The energy is transferred in a non-radiative manner by long-range dipole-dipole interactions of about 10 nm. The FRET efficiency is inversely proportional to the sixth power of the separation distance of the two fluorophores and is therefore very distance dependent. The equation is given by:

$$E_{FRET} = \frac{R_0^6 + r^6}{R_0^6} \quad [2.7]$$

Where R_0 is the distance at which efficiency of energy transfer is 50% and r is the distance between donor and acceptor. For FRET to work, the emission spectrum of the donor needs to overlap with the excitation of the acceptor. Because of the distance dependence, molecular interactions can be confirmed by measuring the wavelength of the emitted light. FRET can be used for analysis of several mechanisms including protein-protein interactions, proteolysis and protein conformational changes (Ishikawa-Ankerhold et al., 2012). The technique was used in this project to measure the degree of vesicle mixing for hybrid vesicles by sonicating FRET-pair labeled vesicles with unlabeled vesicles. The mixing increases the average

distance between labeled head groups and therefore a decrease of the intensity of the fluorescence signal of the acceptor molecule could be measured in a spectrofluorometer.

3

Materials & Methods

In this chapter the materials and methods used in this work are described. Unless stated otherwise all general chemicals were purchased from Sigma-Aldrich (St. Louis, Missouri USA) and all lipids from Avanti Polar Lipids (Alabaster, Alabama USA).

3.1 Preparation of native membrane vesicles

Native membrane vesicles (NMVs) were extracted from green monkey kidney (GMK) "VERO" cells, an established cell line for cultivation of herpes virus in general (Adamiak et al., 2007). The cells were carefully removed from the culture flasks by gently scraping the inside after addition of PBS and lysis buffer (2xPBS, 1 mM EDTA, and protease inhibitor cocktail, Roche) to avoid protease activity and increase cell lysis. The cell solution and additional lysis buffer was added to falcon tubes kept on ice. A small amount of cells was collected from the cell medium by centrifugation (740g for 7 min, 4 °C), the pellets were resuspended in lysis buffer and then added to the remaining cells. The cells were centrifuged for 10 minutes at 1000g and 4 °C to increase the concentration. They were then homogenized with a glass Dounce homogenizer applying more than 30 strokes. The cell solution was centrifuged for another 20 minutes at 740g to remove any non-lyzed material. The resulting pellet was resuspended and homogenized again. The solution was then ultracentrifuged at 50000 RPM and 4 °C for 90 min to finally separate the NMVs from the rest of the cell components. The pellet was finally resuspended in 2×PBS and 20% glycerol. The NMVs were snap frozen with liquid nitrogen and stored at -80 °C.

3.2 Preparation of PEGylated POPC vesicles

Vesicles of 1-palmitoyl-2-oleoyl-sn-glycero-3-phosphocholine (POPC) were modified by including 0.5 mol % polyethylene glycol ceramide (PEG). The vesicles were prepared by dissolving the right ratios of PEG (5000 g/mol, 10 mg/ml) and POPC (10 g/ml) in chloroform. The solution was then dried with N_2 and then dried further under vacuum for about 2 hours. The lipids were rehydrated in PBS buffer (10 mM sodium phosphate, 150 mM sodium chloride at pH 7.5) and extruded 10 times through a 100nm filter (Whatman) forming PEGylated POPC vesicles (PEG_POPC) with an extrusion set (Avanti Polar Lipids).

3.3 Vesicle mixing and FRET analysis

In order to create vesicles that spontaneously rupture forming SLBs, the NMVs were mixed with PEG_POPC to create hybrid vesicles. Ultra-sonication was performed with a bath sonicator (37 kHz, 140W, Elmasonic S40H, Germany). If not stated otherwise, the vesicles were sonicated for 10 minutes at 30 °C. In order to optimize sonication conditions a FRET analysis was done using so-called FRET vesicles (1 mol % Rhodamine labeled 1,2-dioleoyl-sn-glycero-3-phosphoethanolamine (DOPE), 1 mol % Nitrobenzoxadiazole (NBD) labeled DOPE and 98 mol % POPC) mixed with POPC vesicles, see Result section Figure 5. An increased mixing of the FRET vesicles results in a decreased FRET signal because the

non-labeled POPC vesicles dilute the FRET pairs. A volume of 1 µl FRET vesicles (1mg/ml) was mixed with 10 µl POPC vesicles (1mg/ml) and PBS buffer (10 mM sodium phosphate, 150 mM sodium chloride at pH 7.5) was added until a total volume of 60 µl was reached. The solution was then sonicated at different temperatures and times to find the optimal sonication conditions for vesicle mixing. To carry out the fluorometric measurement, an additional 240 µl PBS was added to reach a satisfactory volume for the cuvette.

3.4 Concentration calibration

With a similar approach to determining sonication conditions a calibration curve to approximate vesicle concentration was acquired by sonicating known concentrations of POPC with FRET vesicles and measuring the fluorescence shift from the 590 nm to the 530 nm peak, see result section Figure 6. The calibration curve was performed using 1 µl FRET vesicles (1 mg/ml) sonicated with 2, 4, 8, 16 or 32 µl POPC vesicles (1 mg/ml) and PBS to a total volume of 60 µl. The ratio of the 530 nm and 590 nm fluorescence peaks was plotted against the mol % of FRET vesicles. The resulting calibration curve was a linear equation that is used to estimate the concentration of unknown vesicle samples.

3.5 Fluorometry

The fluorescence was measured with a spectrofluorometer (QM-4/2005 spectrofluorometer, Photon Technology International Inc) with the wavelength spectrum set between 490 and 640 nm. The fluorescence from the donor (530 nm) is expected to increase as the intensity of the acceptor (590 nm) is decreasing. The ratio of the FRET signal was therefore measured at 530 and 590 nm.

3.6 Preparation of sample wells

Cover glasses were cleaned by boiling in 1% Liquinox (Alconox) in water for about 2 hours. The solution was then exchanged to milliQ water and stored in a beaker for maximum 2 days. A piece of polydimethylsiloxane (PDMS) about 1.5x1.5 cm in size with punched holes was then attached to the glass by force and residual glue from tape. The resulting wells hold about 15 µl.

3.7 SLB formation

Depending on the desired composition of the SLBs different volumes of NMVs and PEG_POPC were sonicated, the volume of native membrane material ranged between 12 µl and 18 µl of the total 60 µl meaning a volume percentage of 20-30%. The membranes in the Result section are all consisting of 20 volume % native material. The negative control consisting of only PEG_POPC was also sonicated at the same conditions. To form the SLBs, 10 µl of the vesicle solution was added into each well. The SLBs were allowed to form for 15 minutes and then the wells were gently rinsed with PBS buffer ten times to remove excess vesicles in the bulk.

It is possible to observe the formation of SLBs live through a TIRF microscope by labeling one in 1000 vesicles with rhodamine. The fluorescently labeled vesicles are called tracer vesicles. Upon fusing with the non-labeled lipids in the SLBs the local concentration of fluorophore is drastically decreased and the signal of the tracer vesicles disappears almost immediately. For example, to observe POPC SLB formation 2 µl POPC (1 mg/ml), 1 µl tracer vesicles (2 µg/ml) and 7 µl PBS is mixed giving 0.2 mg/ml POPC vesicles and 0.2 µg/ml tracer vesicles.

3.8 Virus labeling

The concentration of virus was determined by quantitative DNA analysis, assuming that one set of DNA equals one virus particle (Kessler et al., 2000). The HSV-1 KOS and gC deficient strains were labeled with PKH 26 red fluorescent cell linker. The fluorescent material was first diluted 1:9 in ethanol giving a final concentration of 0.1 mM. 6 µl of the diluted PKH 26 was then dissolved in 100 µl diluent C. This solution was incubated for 10 minutes in a solution consisting of 10 µl virus solution and 100 µl diluent C. To prepare a microspin column (GE Healthcare) the liquid was initially centrifuged at 740g for 1 minute, then 300 µl PBS buffer was added and centrifuged at 740g for 2 min, a total of three times. Once ready, the virus solution was centrifuged for 2 minutes at 740g in the prepared microspin column and the labeled viruses were collected. The labeled virus was kept on ice and protected from light.

3.9 Binding inhibition

A binding inhibition experiment was performed with native heparin as an inhibitor. After virus labeling six concentrations (1000, 100, 10, 1, 0.1 and 0.01 µg/ml) of heparin were mixed with the labeled virus particles. The solutions were allowed to incubate for 10 minutes and were then added to the prepared native membrane SLBs in the PDMS wells. They were then allowed to incubate for approximately one hour before imaging. As a positive control the native-like SLB was incubated with viruses without any inhibition. For negative control a POPC SLB was used instead of the native-like membrane and there was no heparin inhibition.

3.10 Total Internal Reflection Fluorescence microscopy

TIRFM was used to study virus binding kinetics. The instrument used was an inverted Nikon Eclipse Ti-E microscope (Nikon Corporation, Japan). An Andor Ixon+ EMCCD camera (Andor Technology, Ireland) and, a 60x magnification oil immersion objective, mercury lamp, and a perfect focus system. 10 µl of the labeled virus is added into the PDMS wells that holds about 5 µl PSB buffer. After about one hour of virus incubation on the SLBs the microscope slide with the PDMS wells was firmly attached to the microscope stage. Green light (TRITC filter) with an exposure time of 100ms was used, effectively exciting the PKH 26 fluorophores. The time interval between shots was either 1 or 15 seconds, this was to reduce the amount of photo bleaching. To image several locations simultaneously the microscope could be programmed to move its stage according to set coordinates.

3.11 Equilibrium-fluctuation analysis

To determine the reaction coefficients for binding and release of the virus particles to the SLBs simultaneously and individually a method is needed to study the kinetics of single particles. The binding frequency, residence time and dissociation of fluorescently labeled HSV-1 particles could be probed with time dependent TIRF microscopy in an assay called equilibrium-fluctuation analysis (EFA). This method determines the kinetic parameters of binding and release at equilibrium conditions. The statistics of binding and release of every particle are extracted from a series of pictures taken with an EMCCD camera coupled to the TIRF microscope. With the TIRF microscope binding events were probed by taking pictures according to a set time interval, this time interval was either one second or 15 seconds. The 15-second movies allowed for better statistics because images could be taken at four separate positions. The image stacks were aligned with a rigid body transformation in ImageJ to correct for movement of the picture associated with the microscope's stage movement. The images were then imported into MatLab (Mathworks, R2015a). This program was used to further analyze the data. A previously written script in MatLab tracks the viruses attaching

and releasing from the surface as well as the residence time of every individual spot. The action of binding, photobleaching and release depends on three intensity threshold defined by the user. The number of frames needed for a particle to be considered firmly bound was also determined; this was typically three frames for the 15-second movies, which is a total of 45 seconds. Particles that were not attached to the surface but disturbed the data because of its movement was manually removed in ImageJ. The approximate reaction coefficients could be determined from the trendline of the association and dissociation plots.

The exponential fit of the particle residence times reveals the dissociation reaction coefficient according to equation [2.3].

The association reaction coefficient is determined from the slope of the cumulative particle association plot, which does not take dissociation into account. This way the dissociation term can be removed from [2.1] giving:

$$\frac{\partial \Gamma(t)}{\partial t} = k_{on} \times C\left(\Gamma_{max} - \Gamma(t)\right) \qquad [3.1]$$

With the assumption that the coverage of receptor is much larger than the coverage of the ligand-receptor complex on the surface, $\Gamma_{max} \gg \Gamma(t)$, [3.1] can be written as:

$$\frac{\partial \Gamma(t)}{\partial t} = k_{on} C \Gamma_{max} \qquad [3.2]$$

This shows that the association rate constant is directly proportional to the rate of coverage of the ligand and therefore this rate can be compared between samples if the ligand and receptor concentrations are identical or known (Gunnarsson et al., 2008). This also means that the association rates of the two HSV-1 strains can be scaled according to their respective virus concentration.

4

Results & Discussion

In this chapter the data from the different kinetic studies done on the HSV-1 and the native membrane SLBs will be presented and discussed. However, first is a section on the characterization of the platform.

4.1 Determination of sonication conditions to form hybrid vesicles

It is generally strived for to get a good mixing of the membrane material and PEG_POPC vesicles resulting in homogenous hybrid vesicles that reliably form SLBs. To determine the optimal conditions for mixing, different sonication settings were investigated. By utilizing FRET paired vesicles the degree of mixing of the native membrane material could be compared between sonication conditions by observing the fluorescence in a common FRET assay. In such an experiment, there is a dip in the 590 nm emission when mixing occurs which means that FRET happens less frequently because the FRET pairs have moved further apart from each other. This also results in an increased fluorescence in the 530 nm peak. In this project; time and temperature were the only parameters explored (see Figure 5).

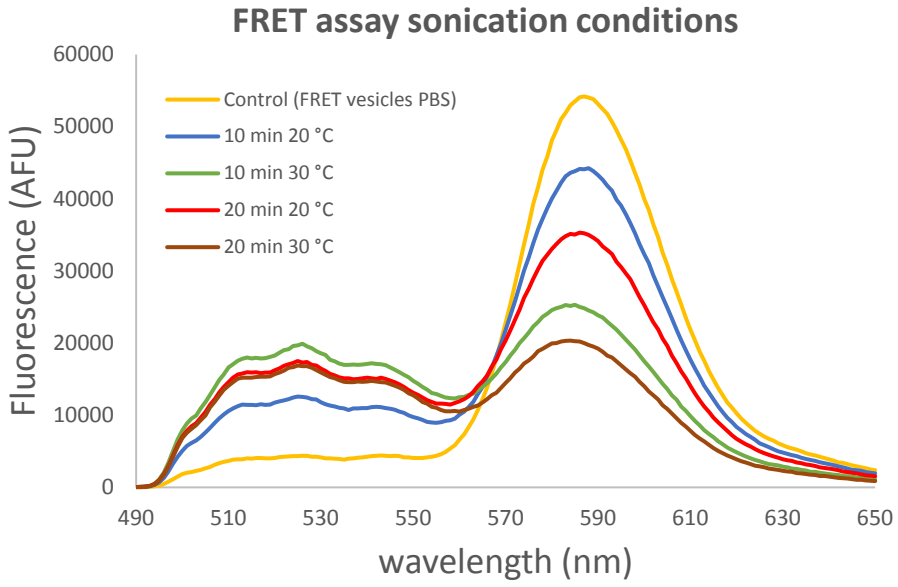

***Figure 5**: FRET assay measurements of FRET labeled vesicles sonicated with native membrane vesicles at four different conditions. The FRET vesicles were sonicated with NMVs in a 1:10 volume ratio. The fluorescent peak at 590 nm is expected to decrease as the FRET vesicles are diluted by the NMVs. From this experiment the condition chosen for the remainder of preparations was determined to be 10 min at 30 °C.*

To minimize the influence of the total fluorescent signal represented by the area under the curve, the ratio between the 530 and 590 nm peaks were compared, see Table 1.

***Table 1**: The ratio of the fluorescent peak value at 530 and 590 nm. The ratio was slightly bigger for 20 min and 30 °C but 10 minutes was used instead because the difference was insignificant. The negative control is only FRET vesicles in PBS.*

Condition	Ratio 530 nm/590 nm
Negative control	0.08
10 min at 20 °C	0.27
10 min at 30 °C	0.78
20 min at 20 °C	0.48
20 min at 30 °C	0.83

The results show that the extent of mixing and hence the 530 nm/590 nm ratio increased with temperature and time. The condition with the highest ratio was 20 min at 30 °C. However, the second highest ratio was only about 6% lower. Because of the substantial sonication time difference and the negligible benefit, the optimal sonication conditions concluded from this experiment were 10 min at 30 °C. The remaining experiments were all performed at these conditions.

4.2 Native membrane material concentration

An approximate determination of the amount of native membrane vesicle material found in the sample provides valuable information in the context of investigating native membrane SLBs and facilitates the comparison across studies. To obtain a quantitative indication of the NMV concentration, a calibration curve was obtained by mixing FRET vesicles and known concentrations of POPC vesicles by sonication. The ratio of the 530 nm and 590 nm fluorescence peaks was plotted against the molar percentage (mol %) of FRET vesicles which yielded a linear relation, see Figure 6.

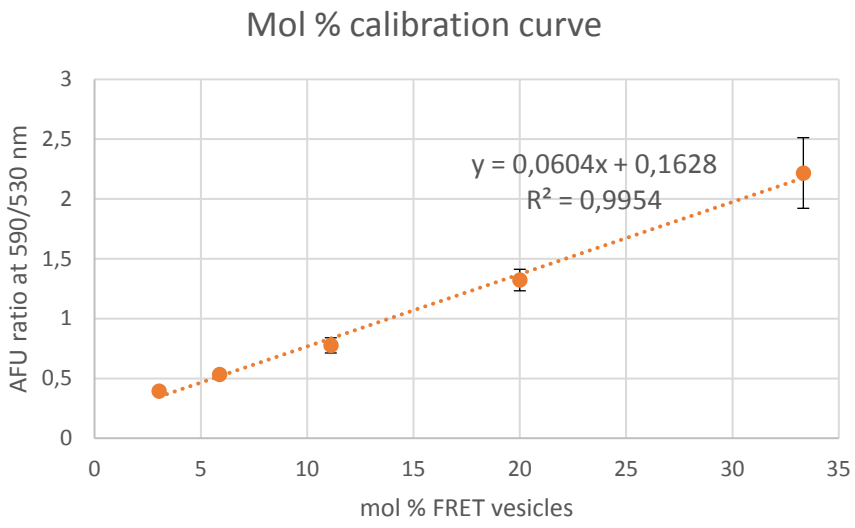

***Figure 6**: FRET vesicles and different concentrations of known POPC vesicle solutions were sonicated. The ratio of fluorescence signal peak values at 590 and 530 nm plotted against the mol % of FRET vesicles. A linear approximation of the data was produced. The linear fit was true to the data with an R^2 value close to 1. The linear relation can give an approximation of the unknown vesicle concentration. Every data point was produced from three repeats.*

With the linear equation approximate concentrations of vesicles could be determined. From this calibration curve the concentration of NMVs in this experiment was estimated to about 0.325 mg/ml, which is quite low but a reasonable yield from the extraction process. Since NMVs are comprised of a vastly complex composition and might very well behave differently compared to POPC vesicles the approximation is not completely reliable, but it provides a rough estimate. Offering an estimate of the concentration makes it much easier to compare data across studies performed on the same cell line. If refined by looking at other more complex vesicles of known concentration the model might yield more precise concentrations. Even though the absolute value may not be correct this technique could provide a relative membrane concentration comparison between samples.

4.3 Binding and release of HSV-1

Determining the kinetic parameters of association and dissociation is vital for the comparison of different interaction conditions, when looking at the effect of inhibitors and more. To probe the binding and release of HSV-1 to the native membrane SLBs, TIRF microscopy was used. The native membrane SLBs were formed and fluorescently labeled viruses were added in solution. Pictures were taken of the bound virus particles with a set time interval. The data was analyzed with a computer program that counts the number of particles bound to the surface and their individual residence time. With the information, association and dissociation could be quantified. The slope of the association curve (Figure 7A) is directly proportional to the association reaction coefficient, k_{on} (Eq 3.2). The dissociation reaction coefficient k_{off} , can be calculated from the exponential fit of the dissociated particles (Eq 2.3), see Figure 7B.

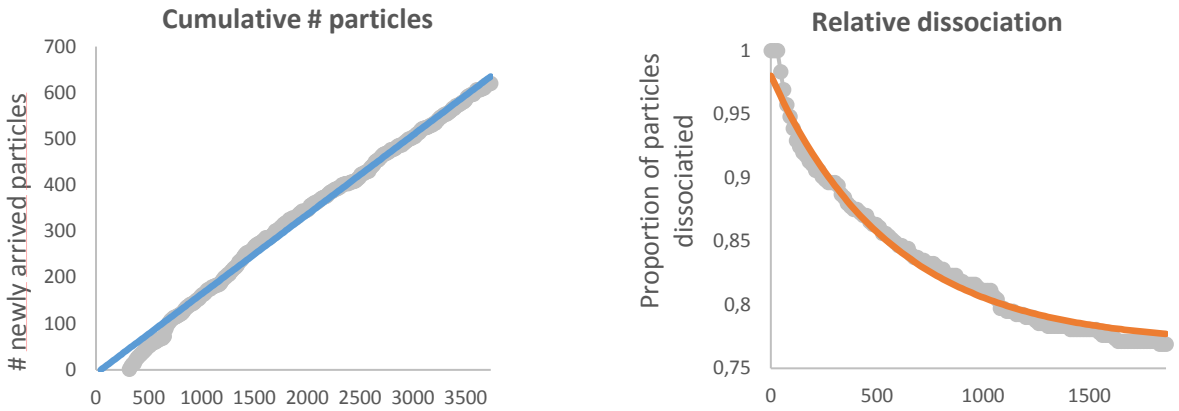

***Figure 7**: (A) The association curve: newly arrived particles are counted during a certain time interval yielding a cumulative plot. The slope of the association curve is proportional to the association reaction coefficient. (B) The dissociation curve: In this instance the numbers are scaled to be relative to the total amount of dissociated particles. The dissociation is determined from the residence time of the particles. The dissociation reaction coefficient can be extracted from the exponential fit.*

Enough data is needed in order to get a clear trend in the association and dissociation plots. This was a problem specifically in the heparin inhibition study because the dissociation events were much rarer compared to association which meant that the short movies of approximately 12 minutes with one second between frames provided too little data to determine the k_{off}. For best statistics long movies of one hour should be taken, this was carried out in the subsequent study on the comparison between the wildtype HSV-1 and a gC deficient strain. These long movies require longer time intervals, in this case 15 seconds, to prevent photobleaching. The

drawback being that faster interactions cannot be recorded. However, this was generally not a limitation in this study.

4.4 Binding kinetics of heparin inhibition

Providing evidence that the platform is functional and also has a specific binding interaction with GAGs is important for the credibility of the following experiments and the continuation of the study. To evaluate if the platform has specific binding interactions with HSV-1 an inhibitor was introduced. Heparin is a sulfated GAG that works as a binding factor to the two major viral attachment glycoproteins gC and gB. The heparin in solution binds competitively with the native sulfated GAGs on the SLBs to the virus glycoproteins. The expected result would reveal a dose-response relationship. If this prevents binding one can conclude that the binding is specific. Furthermore, if the binding kinetics can be measured, the platform could be used to compare different inhibitors. In this experiment the virus particles were premixed with the inhibitor and then added to the SLBs. The time interval between pictures was set to 1 second to reduce the total experimental time; this meant that the kinetics were measured during approximately 12 minutes. A dilution series of six heparin concentrations, positive control (native-like SLB, no inhibition) and negative control (POPC SLB, no inhibition) was tested. The rate of association was determined with equilibrium fluctuation analysis, see Figure 8.

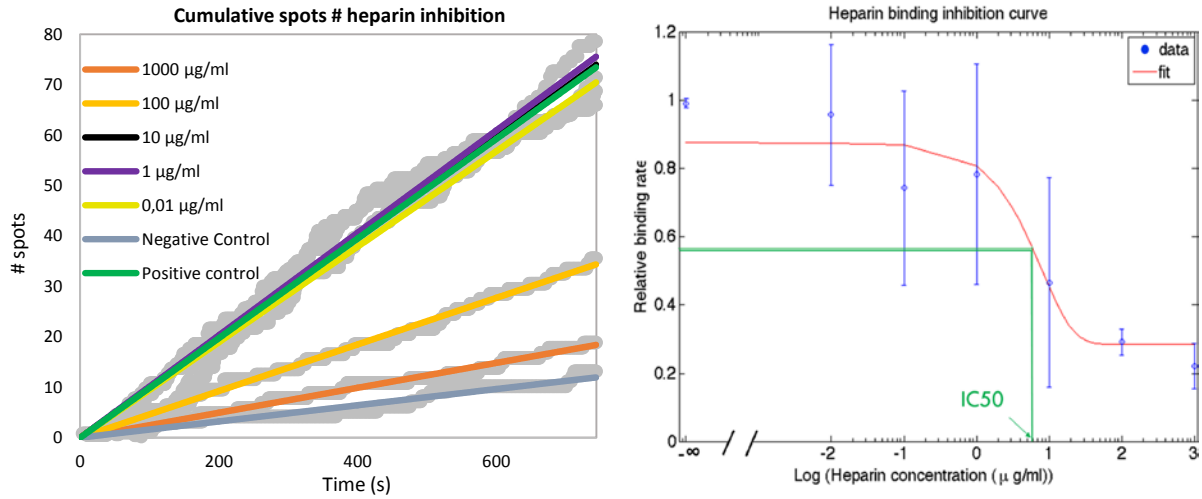

(A) (B)

***Figure 8**: (A) The cumulative number of particles bound to the surface per time. The colored lines are linear approximations of the grayed out data points. The slope is proportional to the association reaction coefficient k_{on}. The highest concentration of heparin (1000 µg/ml) had the lowest k_{on}, but still showed more binding than the negative control. This figure represents the result from a single test. (B) The slope of association curve plotted against the logarithm of the heparin concentration revealed a dose-response relationship. An approximate IC50 value could be achieved from the data. To comprise the data from four repeats an "S" shaped curve fit was performed in MatLab for each data set and all values were scaled to the highest binding rate of the fit.*

It is easily observed that the presence of the heparin is affecting the amount of particles binding to the SLB surface. At low heparin concentration there is not much effect and thus the slope related to the association reaction coefficient is close to the positive control. At higher concentration there are less virus particles binding to the surface and the signal is decreased. One can also see that there was still residual binding to the negative control (PEG_POPC) and this might indicate that there is an unspecific interaction between the native membrane SLBs

and the virus particles or that there might be other interactions with native membrane material unknown to us.

The slope of the association curve was plotted against the heparin concentration and four data sets were combined which made the results easier to visualize. A dose response curve was extracted from the binding inhibition study, see Figure 8B. Although the error is quite large for some data points, one can observe a clear dose response curve from the heparin inhibition. The low binding rates to the PEG_POPC bilayer (~0.12 relative binding rate) compared to the native membrane SLBs (without inhibition) indicate successful incorporation of native membrane material into the SLBs, therefore demonstrating the functionality of the platform. An approximate IC50 value, defined as the concentration at which half of the maximum inhibition is reached, can be determined from the dose-response curve. The IC50 value is a standard way of evaluating the effectiveness of an inhibitor and its determination in this study shows the potential of this system to be used as a screening platform for pharmaceutical targets.

The dissociation constants could not be compared for the heparin inhibition because the data was based on short 12 minute movies that had too few dissociation events. Therefore no statistically significant result on dissociation kinetics could be obtained.

4.5 Binding kinetics comparison wildtype & gC deficient strain

To further test the capability of the platform to measure kinetics and evaluate if the virus attachment is dependent on gC, an experiment was conducted on two different strains of HSV-1. Binding kinetics were compared between the wildtype version of the virus (KOS) and a mutant strain that lacks gC, the major ligand for attachment to surface bound GAGs.

The aim of this part of our study was to compare the binding kinetics of the gC deficient and the wild-type strain using the native-membrane platform and to further study the functionality of this platform. Indeed, specific binding of HSV to the native-like SLB, should be significantly reduced for the gC deficient strain. For this experiment, the two virus strains were treated equally through the whole process: labeling, incubation on the SLBs and imaging with TIRFM. The time interval for acquisition was set to 15 seconds in this case, allowing for an improvement of data statistics over the short time series and acquisition of dissociation data. The association plot from a representative data set is shown described in Figure 9A, the combined results are presented in Figure 9B.

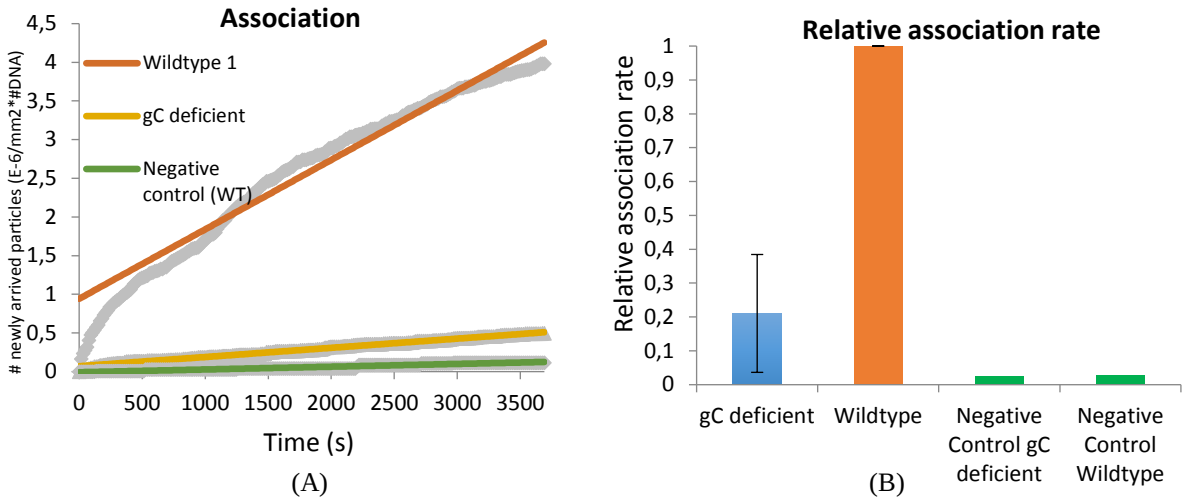

(A) (B)

***Figure 9**: (A) Cumulative number of particles bound to native SLBS for HSV-1 wilt type (red) and gC-lacking mutant (yellow) together with a control experiment (Wild type on POPC, green). There is a very large difference between the gC deficient strain and the wildtype. The negative control is also significantly lower. The colored lines are linear approximations of the grayed out data points. (B) The relative association rate of the wildtype and gC deficient strain. The difference in virus concentrations of the samples was accounted for. There was a very significant difference between the two strains. The two negative controls have no repeats and therefore lack error bars, the other data is combined from three tests.*

By combining three data sets the relative association rate could be compared between the two strains. The association rate for the gC deficient strain was only about one fifth compared to the wildtype. This result was quite expected because previous findings show that the infectivity of the virus could reduce as much as ten-fold for gC deficient strains (Herold et al., 1991). In addition to this, it was observed that the virus particles are still binding more to the gC deficient strain compared to the negative control. This is not surprising because the glycoprotein B on the surface of the gC deficient strain is still present and it is also known to bind to sulfated GAGs, initiating virus attachment. Worth mentioning though is that at this stage we cannot exclude that there might be aggregation of the gC viral particles. Therefore it is difficult to compare the two strains because the contribution of aggregation on binding kinetics is unknown. If the particles aggregate they might form multiple bonds per particle thus decreasing the dissociation.

The dissociation constant was determined from the exponential fit of the dissociated particles, see Figure 10A. There were enough dissociation events during this experiment to assess the dissociation rate. The relative dissociation constant for the gC deficient strain was significantly higher than the wildtype meaning that the gC deficient virus particles release faster from the surface. Taken together, it can be concluded that the gC deficient virus particles are less likely to bind to the SLBs, which is in line with the study on association kinetics. Also, they have a tendency to release faster from the surface compared to wildtype.

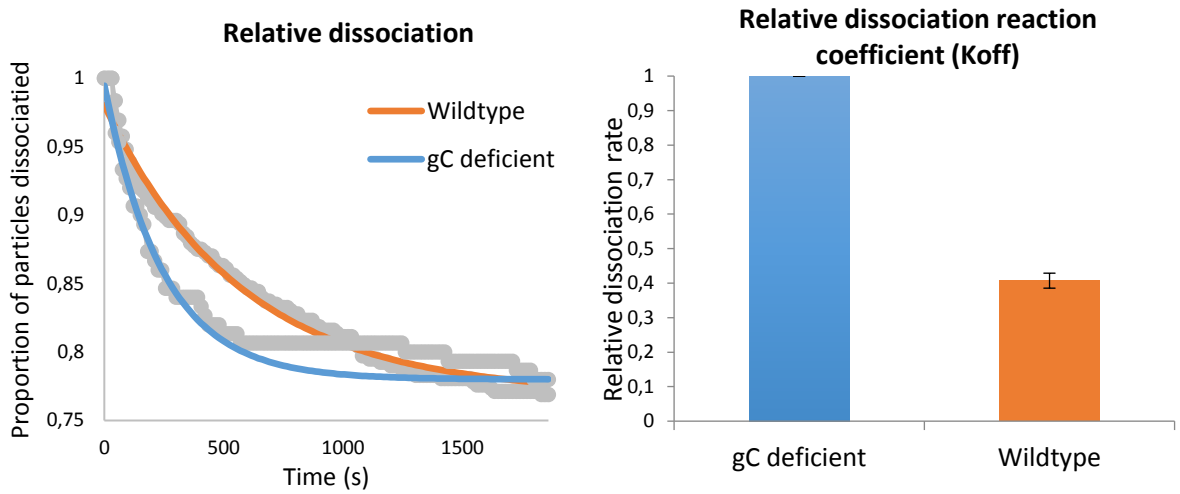

(A) (B)

***Figure 10**: (A) The relative dissociation of virus particles from the SLB surface. The dissociation is determined from the residence time of the virus particles on the SLBs and the dissociation reaction coefficient was determined from the exponential fit of the data. The gray are data points. (B) Relative dissociation reaction coefficient. There was a very significant difference K_{off} between the two strains. The wildtype HSV-1 has a lower dissociation reaction coefficient compared to the gC deficient strain meaning that the virus particles have longer residence times on the surface. The data is based on three repeats.*

From the association results on heparin inhibition and the HSV-1 strain comparison it is possible to determine the association reaction coefficient if the surface coverage of the binding factors and the ligand concentration is known, described by the equation [3.2]. Moreover, as defined in chapter 2.2 the dissociation constant (K_D) could also be determined from the association and dissociation reaction coefficients. This constant can be compared to experiments performed with other systems involving different inhibitors allowing for better comparisons between studies.

5

Conclusions & Outlook

In this project, the native membrane SLBs made from the GMK cell line was successfully constructed. With this platform, it was possible to probe the association and dissociation events of HSV-1 to the native material on the native-like SLB surface. Binding kinetics could be compared to evaluate the inhibition efficacy of heparin and the binding behavior of different strains of HSV-1 with equilibrium fluctuation analysis. The comparison of binding kinetics between the wildtype and the gC deficient strain revealed that the gC deficient strain had lower association and a dissociation coefficient higher compared to the wildtype, which was expected given that gC is the main attachment glycoprotein of HSV-1. The inhibitory study with heparin showed a characteristic dose dependent inhibitory response, demonstrating successful inhibition of the HSV interaction.

The results from the association and the dissociation kinetics investigation strongly suggest that the platform contains functional native membrane material that interacts with the viruses. Additionally, the EFA is capable of determining the kinetics of binding and release based on single particle analysis. It is also possible to compare inhibitors or other drugs based on the dose-response relationship and the resulting IC50 value. This platform is a new approach to screening for antiviral drugs that is simpler and cheaper than cell-based systems. In addition, it introduces parts of the complexity of a native system, therefore being more nature-like than single ligand-receptor systems. Another advantage is that this platform can suit a wide range of applications, since it can be used with different cell lines (Pace et al., 2015). Furthermore, it allows the use of surface-sensitive techniques, which is very difficult in cell-based screening systems.

To further test the platform, one could investigate a larger variety of antiviral drug candidates to probe their inhibitory binding effects. Another direction is to incorporate other cell lines into the native-like SLBs that are suitable for the investigation of other viruses. This could provide additional evidence that the platform could be used as a screening system for multiple viruses. One could also use the platform to study the role of GAGs by incorporating modified cells that are GAG deficient, making it easy to study their impact by comparing it to a cell line rich in GAG attachment factors. Although progress has been made, the platform meets many challenges on the way to becoming a standard assay for drug screening. Preservation of the properties of the native membrane SLBs for a longer time would greatly enhance the data acquisition during imaging and thus the statistical significance. This also applies to the reliability and reproducibility of native membrane SLB formation and TIRFM probing. The platform could be further characterized by investigating the structure of the native-like SLBs in detail by topographic AFM analysis. At this point we are unsure exactly how the native material position itself within the membrane and the topography might offer this information. A key goal for the future of the platform is to have an on chip design capable of running

screening in high throughput. The screening system does have a lot of potential and looking beyond the horizon it is without a doubt a contender for screening the next generation of antiviral drugs not only for HSV-1 but other viruses as well. With the knowledge that the platform and the procedure of forming a native membrane SLB is working, the method could be applied to other cells and pathogens as a screening tool for the investigation of tomorrows medicines and vaccines.

Acknowledgements

First off, a big thanks to all of the people at the *biological physics group*, you are all such friendly and knowledgeable people that keep your spirits up.

I would like to express my gratitude to my supervisor *Nadia* for helping me out with basically everything during my master's thesis project, you really made this work a whole lot better. Many thanks to my examiner *Marta* for all of the insightful comments that helped me along the way and for just being available despite having a lot of other work to do. Thank you *Hudson* for introducing me to the lab environment and *Olov* for assisting me with MatLab.

A big thanks to my *family and friends* and especially *Hanna* for supporting me throughout this project and my whole education, for this I am forever grateful.

Bibliography

ADAMIAK, B., EKBLAD, M., BERGSTROM, T., FERRO, V. & TRYBALA, E. 2007. Herpes simplex virus type 2 glycoprotein G is targeted by the sulfated oligo- and polysaccharide inhibitors of virus attachment to cells. *J Virol,* 81**,** 13424-34.

BALLY, M., BAILEY, K., SUGIHARA, K., GRIESHABER, D., VOROS, J. & STADLER, B. 2010. Liposome and lipid bilayer arrays towards biosensing applications. *Small,* 6**,** 2481-97.

DAHLIN, A. B. 2012. Kinetics of Molecular Binding to Surfaces. *In:* DAHLIN, A. B. (ed.) *Plasmonic Biosensors: An Integrated View of Refractometric Detection.* Amsterdam: IOA Press.

GANDHI, N. S. & MANCERA, R. L. 2008. The structure of glycosaminoglycans and their interactions with proteins. *Chem Biol Drug Des,* 72**,** 455-82.

GOZEN, I. & JESORKA, A. 2012. Instrumental methods to characterize molecular phospholipid films on solid supports. *Anal Chem,* 84**,** 822-38.

GUNNARSSON, A., JONSSON, P., MARIE, R., TEGENFELDT, J. O. & HOOK, F. 2008. Single-molecule detection and mismatch discrimination of unlabeled DNA targets. *Nano Lett,* 8**,** 183-8.

HEROLD, B. C., WUDUNN, D., SOLTYS, N. & SPEAR, P. G. 1991. Glycoprotein C of herpes simplex virus type 1 plays a principal role in the adsorption of virus to cells and in infectivity. *J Virol,* 65**,** 1090-8.

ISHIKAWA-ANKERHOLD, H. C., ANKERHOLD, R. & DRUMMEN, G. P. 2012. Advanced fluorescence microscopy techniques--FRAP, FLIP, FLAP, FRET and FLIM. *Molecules,* 17**,** 4047-132.

JOSIC, D. & CLIFTON, J. G. 2007. Mammalian plasma membrane proteomics. *Proteomics,* 7**,** 3010-29.

KARRE, P. R. & COOPER, G. B., 2ND 2011. The azygos lobe and vein: interesting and typical clinical image. *BMJ Case Rep,* 2011.

KESSLER, H. H., MUHLBAUER, G., RINNER, B., STELZL, E., BERGER, A., DORR, H. W., SANTNER, B., MARTH, E. & RABENAU, H. 2000. Detection of Herpes simplex virus DNA by real-time PCR. *J Clin Microbiol,* 38**,** 2638-42.

KOSHY, C. & ZIEGLER, C. 2015. Structural insights into functional lipid-protein interactions in secondary transporters. *Biochim Biophys Acta,* 1850**,** 476-87.

KRUG, A., LUKER, G. D., BARCHET, W., LEIB, D. A., AKIRA, S. & COLONNA, M. 2004. Herpes simplex virus type 1 activates murine natural interferon-producing cells through toll-like receptor 9. *Blood,* 103**,** 1433-7.

LIN, W. C., BLANCHETTE, C. D., RATTO, T. V. & LONGO, M. L. 2006. Lipid asymmetry in DLPC/DSPC-supported lipid bilayers: a combined AFM and fluorescence microscopy study. *Biophys J,* 90**,** 228-37.

LODISH, H. F. & DARNELL, J. E. 2000. Viruses: Structure, Function, and Uses. *In:* LODISH, H. F. & DARNELL, J. E. (eds.) *Molecular cell biology* 4th ed. New York: W.H. Freeman.

LOOKER, K. J., MAGARET, A. S., MAY, M. T., TURNER, K. M., VICKERMAN, P., GOTTLIEB, S. L. & NEWMAN, L. M. 2015. Global and Regional Estimates of Prevalent and Incident Herpes Simplex Virus Type 1 Infections in 2012. *PLoS One,* 10**,** e0140765.

MOLLER, I. & SEEGER, S. 2015. Solid supported lipid bilayers from artificial and natural lipid mixtures - long-term stable, homogeneous and reproducible. *Journal of Materials Chemistry B,* 3**,** 6046-6056.

PACE, H., SIMONSSON NYSTROM, L., GUNNARSSON, A., ECK, E., MONSON, C., GESCHWINDNER, S., SNIJDER, A. & HOOK, F. 2015. Preserved transmembrane protein mobility in polymer-supported lipid bilayers derived from cell membranes. *Anal Chem,* 87**,** 9194-203.

RICHARDS, M. J., HSIA, C. Y., SINGH, R. R., HAIDER, H., KUMPF, J., KAWATE, T. & DANIEL, S. 2016. Membrane Protein Mobility and Orientation Preserved in Supported Bilayers Created Directly from Cell Plasma Membrane Blebs. *Langmuir*.

RICHTER, R., MUKHOPADHYAY, A. & BRISSON, A. 2003. Pathways of lipid vesicle deposition on solid surfaces: a combined QCM-D and AFM study. *Biophys J,* 85**,** 3035-47.

RICHTER, R. P. & BRISSON, A. R. 2005. Following the formation of supported lipid bilayers on mica: a study combining AFM, QCM-D, and ellipsometry. *Biophys J,* 88**,** 3422-33.

ROSS, S., SCHWARTZ, S., FELLERS, T. & DAVIDSON, M. 2015. *Total Internal Reflection Fluorescence (TIRF) Microscopy* [Online]. MicroscopyU. Available: http://www.microscopyu.com/articles/fluorescence/tirf/tirfintro.html [Accessed May 20 2016].

SIMONSSON, L., GUNNARSSON, A., WALLIN, P., JONSSON, P. & HOOK, F. 2011. Continuous lipid bilayers derived from cell membranes for spatial molecular manipulation. *J Am Chem Soc,* 133**,** 14027-32.

SPEAR, P. G. 2004. Herpes simplex virus: receptors and ligands for cell entry. *Cell Microbiol,* 6**,** 401-10.

VAN MEER, G., VOELKER, D. R. & FEIGENSON, G. W. 2008. Membrane lipids: where they are and how they behave. *Nat Rev Mol Cell Biol,* 9**,** 112-24.

YAMAMURA, H., SUZUKI, Y. & IMAIZUMI, Y. 2015. New light on ion channel imaging by total internal reflection fluorescence (TIRF) microscopy. *J Pharmacol Sci,* 128**,** 1-7.

YU, X., SHAH, S., LEE, M., DAI, W., LO, P., BRITT, W., ZHU, H., LIU, F. & ZHOU, Z. H. 2011. Biochemical and structural characterization of the capsid-bound tegument proteins of human cytomegalovirus. *J Struct Biol,* 174**,** 451-60.